PHILOSOPHICAL TRANSACTIONS A

rsta.royalsocietypublishing.org

Research

Article submitted to journal

Subject Areas:
wave motion, applied mathematics, differential equations

Keywords:
Wiener–Hopf equations, Riemann-Hilbert problem, iterative methods, scattering, n-part boundaries

Author for correspondence:
Matthew Priddin
e-mail: mjp98@cam.ac.uk

Applying an iterative method numerically to solve $n \times n$ matrix Wiener–Hopf equations with exponential factors

Matthew J. Priddin[1], Anastasia V. Kisil[2] and Lorna J. Ayton[1]

[1]DAMTP, University of Cambridge, Cambridge, CB3 0WA, UK [2]Department of Mathematics, The University of Manchester, Manchester, M13 9PL, UK

This paper presents a generalisation of a recent iterative approach to solving a class of 2×2 matrix Wiener–Hopf equations involving exponential factors. We extend the method to square matrices of arbitrary dimension n, as arise in mixed boundary value problems with n junctions. To demonstrate the method we consider the classical problem of scattering a plane wave by a set of collinear plates. The results are compared to other known methods. We describe an effective implementation using a spectral method to compute the required Cauchy transforms. The approach is ideally suited to obtaining far-field directivity patterns of utility to applications. Convergence in iteration is fastest for large wavenumbers, but remains practical at modest wavenumbers to achieve a high degree of accuracy.

1. Introduction

The Wiener–Hopf technique [1] provides a powerful tool to approach varied problems such as the solution of integral equations and random processes. Applications may so be found in such diverse fields as aeroacoustics [2], metamaterials [3], geophysics [4], crack propagation [5] and financial mathematics [6].

The mathematical problem underlying the Wiener–Hopf technique may be simply stated: find functions that are analytic in adjacent (or overlapping) regions of a complex manifold that satisfy a prescribed jump condition at their common boundary.

THE ROYAL SOCIETY PUBLISHING

Often, as in this work, the manifold is the complex plane $\alpha \in \mathbb{C}$, and the regions are the upper and lower half-planes, respectively $\mathcal{D}^+ = \Im(\alpha) > -c$ and $\mathcal{D}^- = \Im(\alpha) < c$ where c is an arbitrary small constant. The jump between two unknown vector functions is described by an equation

$$\boldsymbol{K}(\alpha)\boldsymbol{\Psi}_-(\alpha) + \boldsymbol{\Psi}_+(\alpha) = \boldsymbol{F}(\alpha) \tag{1.1}$$

valid on some strip $-c < \Im(\alpha) < c$, where $\boldsymbol{K}(\alpha)$ is a known matrix function and $+$ and $-$ decorations denote analyticity in the upper and lower half-planes respectively.

The classical Wiener–Hopf technique exploits the analytic structure of the problem by requiring a special multiplicative factorisation of the kernel $\boldsymbol{K}$ into two parts $\boldsymbol{K} = \boldsymbol{K}^-\boldsymbol{K}^+$, each analytic and zero-free in one of the adjacent regions. Such a factorisation has been long known to exist, but generic, stable and constructive approaches are unknown [7]. The stability and well-posedness of the problem rests on certain invariants of the matrix kernel $\boldsymbol{K}$, the *partial indices*, though the only general method to determine these is to solve the hard problem of finding a factorisation [8,9]. We note that in this paper we do not find the matrix factorisation and hence do not determine the partial indices (we know of no results of how to find the partial indices for our class of matrix Wiener-Hopf problems). However, since the class of matrix functions for which our method applies results from well-posed physical problems we believe it should be stable under small perturbations. These difficulties surrounding matrix factorisation mean that in practice it is typical to resort to approximate methods: approximating the matrix, $\boldsymbol{K}$, by one more easily factored, either exploiting a small parameter perhaps associated with a particular physical regime [10,11], or a suitable approximation space as in Padé approximation [12]. One might also undertake the factorisation process by 'singularity removal': introducing functions defined to additively remove the singularities, solving the Wiener–Hopf equation and if necessary subsequently determining any unknown parameters of these functions by enforcing this removal, perhaps approximately [13,14].

When solving mixed boundary value problems using the Wiener–Hopf technique the number of unknown functions is associated with the number of distinct boundary sections on which boundary values must be found. Therefore the solution of matrix problems is vital to exploit the Wiener–Hopf technique to solve physical problems involving multiple changes in boundary condition. Despite its importance, as discussed above, there are sparse methods available to solve general matrix Wiener–Hopf problems [8,9,15]. In addition, much of the existing literature is concerned with the factorisation of 2×2 matrices, leaving the more general and challenging case of $n \times n$ matrix functions relatively unexplored [16–18] (especially where $n > 4$). Exponential factors in the matrix kernel, often associated with the displacement between boundary junctions, pose particular difficulty in part due to their non-factorability. Previous works have considered the restricted cases of 2×2 matrix Wiener–Hopf problems with exponential factors [19,20] and $n \times n$ Riemann–Hilbert problems with meromorphic coefficients [21]. A numerical Riemann–Hilbert formulation [22] has been recently adapted to solve classical Wiener–Hopf problems [23] and certain problems involving exponential factors [24], each relying on the choice of a suitable basis. The numerous potential applications of $n \times n$ Wiener–Hopf problems involving exponential factors underlines the importance of developing suitable methods [25,26].

This paper helps to fill this gap by extending the use of the iterative Wiener–Hopf method introduced in [20] for the two dimensional matrix problem to n dimensions. This method has the particular attraction that each step may permit a physically meaningful interpretation. The two dimensional method has found applications in aeroacoustic [27] and crack propagation problems [28]. In the former, aeroacoustic scattering from a finite porous extension to a rigid trailing edge, each Wiener–Hopf factorisation was undertaken by brute force. In the latter, a crack propagation problem built on the application of the Wiener–Hopf technique in fracture mechanics pioneered in numerous works by Slepyan [29,30]. Importantly, by implementing an effective numerical factorisation procedure based on techniques presented in [22,31–33] this paper shows that this method provides a practical and fast procedure for solving problems involving larger $n \times n$ matrices.

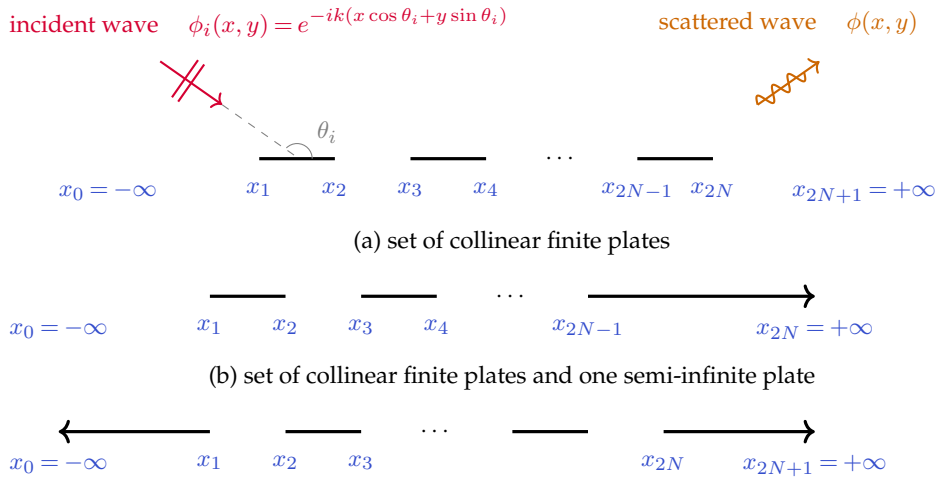

(a) set of collinear finite plates

(b) set of collinear finite plates and one semi-infinite plate

(c) set of apertures in an infinite plate (collinear finite plates and two semi-infinite plates)

Figure 1: Scattering of a plane wave by a set of collinear plates. The set of plates may extend a finite length in (a) none, (b) one or (c) both of the positive and negative x directions.

This new numerical approach is readily applicable to scattering by a set of collinear plates, such as the case of several finite plates shown in figure 1a. This class of geometries encompasses a number of practical and canonical problems, and will be the focus of this paper to demonstrate the iterative method. The Sommerfeld diffraction problem of scattering by a half-plane presents the prototypical scattering model. It is the classical example to introduce the Wiener–Hopf technique [1], dealing with both an unbounded domain and the sharp material junction. The diffraction of a wave by one finite plate (two junctions) has been extensively studied [34–36], but the case of two plates is much harder. Scattering by more than two plates has been explicitly considered using Wiener–Hopf but neglecting edge interactions in [37,38], analytically generalising special functions [39] and numerically in [33,40,41]. Another interesting rigorous approach is to reduce the n-plate problem to the solution of a simple ordinary differential equation [42], here the practical difficulty lies in finding some constant parameters of this ODE. A common theme in many approaches is the successive treatment of diffraction events to yield Schwarzschild diffraction series; our implementation may be interpreted as recovering a diffraction series solution in the spectral domain (Fourier space). The fact that the proposed method is devised in the spectral domain rather than in the physical space is key. This allows to take advantage of the singularity structures of the kernel in the complex plane and hence perform hundreds rather than one or two iterations, see Section 3(c). Significantly, the proposed method applies to some Wiener-Hopf problems arising in crack propagation or Lévi processes, which are not related to diffraction and where a Schwarzschild diffraction series approach would not be a natural choice.

General numerical boundary based methods, that avoid the need for Wiener–Hopf factorisation, can provide effective solutions to scattering problems from convex sets of objects, though typically these require a linear growth in degrees of freedom with increasing wavenumber [33]. This growth may be reduced to at worst logarithmic type by considering a hybrid numerical-asymptotic (HNA) approach where the basis used is supplemented by appropriately chosen oscillatory functions, as proposed in [40]; moreover numerical experiments suggest wavenumber independence. There are however three key attractions of the proposed approach using the Wiener–Hopf technique in comparison to numerical approaches based on Green's functions: first the approach may be readily applied to semi-infinite geometries, second the asymptotic far-field directivity may be naturally recovered by a single function evaluation, and thirdly, in contrast to

unspecialised numerical approaches, it is well-suited to large wavenumbers. We shall illustrate each of these attractions in this paper through various collinear plate setups.

This paper is structured as follows: we first introduce the class of Wiener–Hopf problems to be solved in Section 2 by considering mixed boundary value problems associated with scattering by collinear rigid plates. Section 3 develops the iterative method for $n \times n$ matrix problems, and describes the numerical implementation employed. Results for the distinct canonical cases of collinear rigid plates are presented in Section 4 and consider convergence in Section 5, indicating advantages of this new method for certain problems over alternative approaches.

2. Matrix Wiener–Hopf problem for scattering by collinear plates

In this section we consider how a class of matrix Wiener–Hopf problems motivating the iterative method arise from mixed boundary value problems involving scattering by collinear rigid plates.

(a) Scattering by collinear rigid plates

The concrete example in mind throughout this paper is that of the scattering of an acoustic wave by collinear rigid (sound-hard) plates located along $y = 0$. We distinguish three cases: (a) where all plates have finite extent, (b) exactly one has semi-infinite extent and (c) two have semi-infinite extent, as illustrated in figure 1.

We suppress an implicit time dependence $e^{-i\omega t}$ and write the total wave field as the sum of a scattered field ϕ and an incident field ϕ_i. We focus on the case of a plane wave incident at an angle θ_i to the positive x axis

$$\phi_i(x, y) = e^{-ikx\cos\theta_i - iky\sin\theta_i} \tag{2.1}$$

The scattered field ϕ is required to solve the Helmholtz equation

$$\left(\nabla^2 + k^2\right)\phi = 0 \tag{2.2}$$

away from the plates, $\mathbb{R}^2 \setminus \Lambda$, where Λ is the set of points describing the location of the plates.

Boundary conditions We impose boundary conditions on the scattered field ϕ at $y = 0$ to ensure no penetration of the total field through the rigid (sound-hard) plates, and continuity elsewhere:

$$\frac{\partial \phi}{\partial y} = -\frac{\partial \phi_i}{\partial y} \quad (x, y) \in \Lambda \tag{2.3a}$$

$$[\phi] = \left[\frac{\partial \phi}{\partial y}\right] = 0 \qquad (x, y) \in \mathbb{R}^2 \setminus \Lambda \tag{2.3b}$$

Here $[\cdot]$ denotes the jump in $\cdot$. The scattered solution ϕ is also required to satisfy the Sommerfeld radiation condition for outgoing waves at infinity,

$$r^{-1/2}\left(\frac{\partial \phi}{\partial r} - ik\phi\right) \to 0, \quad \text{where } r = \sqrt{x^2 + y^2} \tag{2.4}$$

and edge conditions in order to achieve the least singular solution

$$\phi(x, 0) \to c_m \qquad \text{as } x \to x_m \tag{2.5a}$$

$$\frac{\partial \phi(x, 0)}{\partial y} \to d_m x^{-1/2} \qquad \text{as } x \to x_m \tag{2.5b}$$

where c_m and d_m are constants [1]. Finally, the nature of this problem means the scattered field is required by symmetry to be an odd function of y, which allows us to restrict attention to $y > 0$.

General solution To apply the Wiener–Hopf technique we proceed in the standard manner by first Fourier transforming in the x variable:

$$\Phi(\alpha, y) = \int_{-\infty}^{\infty} \phi(x, y) e^{i\alpha x} \, \mathrm{d}x \tag{2.6}$$

Imposing decay as $|y| \to \infty$, we find that the x-Fourier transform $\Phi(\alpha, y)$ of a solution $\phi(x, y)$ satisfying the governing equation (2.2) along $(-\infty, \infty)$ may be written

$$\Phi(\alpha, y) = \mathrm{sgn}(y)\Phi(\alpha, 0+)e^{-\gamma(\alpha)|y|} \tag{2.7}$$

where $\gamma(\alpha) = \sqrt{\alpha^2 - k^2}$, having used the fact that the scattered field ϕ is anti-symmetric in y. The branch cuts are taken to be the rays $\{\alpha = \pm k \pm is : 0 < s < \infty\}$ parallel to the imaginary axis. We note from the form of this solution (2.7) that

$$\Phi'(\alpha, 0+) + \gamma(\alpha)\Phi(\alpha, 0+) = 0 \tag{2.8}$$

where $\Phi' \equiv \frac{\partial \Phi}{\partial y}$. This equation relates integral transforms of boundary values, as may be generically found for separable equations by constructing the global relation [41]. To formulate a Wiener–Hopf problem we view this equation as describing jump problem between analytic functions, as described in the next section.

To recover the physical scattered field $\phi(x, y)$ from $\Phi(\alpha, y)$ we invert the x-Fourier transform:

$$\phi(x, y) = \frac{\mathrm{sgn}(y)}{2\pi} \int_{-\infty}^{\infty} \Phi(\alpha, 0+) e^{-i\alpha x - \gamma(\alpha)|y|} \, \mathrm{d}\alpha \tag{2.9}$$

Working in polar coordinates (r, θ) we define the directivity $D(r, \theta) = |\phi(r, \theta)|$. In the limit $r \to \infty$ the leading order term may be found by the method of steepest descent: the directivity for each observer angle then corresponds to a single evaluation of the spectral function Φ at the saddle point $\alpha = -k\cos\theta$. If all plates are of finite extent then ϕ contains no reflected waves, and we may define the far-field directivity $D_\infty(\theta)$ by

$$D_\infty(\theta) = \lim_{r \to \infty} r^{1/2} D(r, \theta) \tag{2.10}$$

We now formulate a Wiener–Hopf problem associated with this class of physical problems.

(b) Formulating the Wiener–Hopf problem

The plate endpoints provide n junctions at which the boundary condition on $y = 0$ to be imposed changes as we cross from a plate to a gap. These junctions, together with $\pm\infty$, yield a partition of the real line $\{x_m | m = 0, \ldots, n+1\}$ with $x_0 = -\infty$ and $x_{n+1} = +\infty$. The boundary conditions provide piecewise relations for boundary values (for instance Dirichlet or Neumann data) on intervals $[x_m, x_{m+1}]$. We so define the *partial range* Fourier transform along each interval $[x_m, x_{m+1}]$ of a function $v(x)$ by

$$V_m = \int_{x_m}^{x_{m+1}} v(x) e^{i\alpha x} \, \mathrm{d}x \tag{2.11}$$

The spectral relation (2.8) and boundary conditions (2.3) now provide an equation relating the unknown data v on each boundary segment, which is permitted to be a linear combination of Dirichlet and Neumann data for that segment, and takes the form

$$\eta_0(\alpha)V_0(\alpha) + \eta_1(\alpha)V_1(\alpha) + \cdots + \eta_n(\alpha)V_n(\alpha) = F(\alpha) \tag{2.12}$$

where V_m is the Fourier transform of such an unknown data value along $[x_m, x_{m+1}]$, $\eta_m(\alpha)$ are known functions and F some known sum of transformed boundary conditions. Equation (2.12) now becomes the focus of our attention, where the V_m must be found in order to solve for $\Phi(\alpha, 0+)$ and so determine the scattered field. For the subsequent analysis $\eta_m(\alpha)$ are assumed to have at worst algebraic growth as $|\alpha| \to \infty$ and branch cut and pole singularities, and without loss of generality we suppose $\eta_0 = 1$.

For the particular case of collinear N collinear finite rigid plates we take the transforms of the unknown data to be of Neumann data away from plates and Dirichlet on plates. This gives

$$V_{2m-1} = \int_{x_{2m-1}}^{x_{2m}} \frac{\partial \phi}{\partial y}(x,0+)e^{i\alpha x}\,\mathrm{d}x, \quad V_{2m} = \int_{x_{2m}}^{x_{2m+1}} \phi(x,0+)e^{i\alpha x}\,\mathrm{d}x \tag{2.13}$$

whence the Fourier transform of the boundary conditions (2.3) may be written as

$$V_{2m-1}(\alpha) = F_{2m-1}(\alpha) \tag{2.14a}$$

$$V_{2m}(\alpha) = 0 \tag{2.14b}$$

where each F_{2m-1} is given by the partial Fourier transform of the known value $-\frac{\partial \phi_i}{\partial y}(x,0+)$ along $[x_{2m-1}, x_{2m}]$. Substituting the expressions (2.14) into (2.8) yields the spectral equation

$$0 = \sum_{m=1}^{N} \left(\gamma(\alpha)V_{2m-1}(\alpha) + F_{2m-1}(\alpha)\right) + \sum_{m=0}^{N} V_{2m}(\alpha) \tag{2.15}$$

The necessary modifications for cases involving a semi-infinite plate extending to $\pm\infty$ follow naturally. Moreover, if the sound-hard boundary condition (2.3*a*) on each plate is replaced by a Robin boundary condition of the form $\frac{\partial \phi}{\partial y} - \frac{\mu}{2}[\phi] = f$, then equation (2.15) is simply modified by the substitution $\gamma \to \gamma + \mu$ such that $\eta_{2m} = 1$, $\eta_{2m-1} = \gamma + \mu$ and V and F are unchanged from (2.15).

With the Wiener–Hopf method in mind, we wish to define the regularity of the unknown functions V_m as plus or minus, respectively denoting analyticity and at worst algebraic growth in $\mathcal{D}^+ = \Im(\alpha) > -c$ and $\mathcal{D}^- = \Im(\alpha) < c$ respectively; these domains emerge from the analyticity of the partial range Fourier transform. The large $|\alpha|$ asymptotics of each partial range transform may be inferred from the exponential shift due to the interval endpoints and the physical solution behaviour near the junction (2.5) by the Abelian theorems [1]. For instance, if V_m corresponds to a partial Fourier transform of ϕ, then the requirement of integrable energy at the edge implies that

$$e^{-i\alpha x_m} V_m = \mathcal{O}(\alpha^{-1/2}) \quad |\alpha| \to \infty \quad \Im(\alpha) > 0 \tag{2.16a}$$

$$e^{-i\alpha x_{m+1}} V_m = \mathcal{O}(\alpha^{-1/2}) \quad |\alpha| \to \infty \quad \Im(\alpha) < 0 \tag{2.16b}$$

This motivates the definition of the plus and minus functions $\Psi_+^{(m)}$ and $\Psi_-^{(m)}$ for $1 \le m \le n$,

$$\Psi_+^{(m)} = e^{-i\alpha x_m} V_{m+1}, \quad \Psi_-^{(m)} = e^{-i\alpha x_m} V_m \tag{2.17}$$

Note that this definition means that $e^{i\alpha(x_m - x_{m+1})}\Psi_+^{(m)} = \Psi_-^{(m+1)}$, so all unknown finite range transforms may be associated with an entry in $\boldsymbol{\Psi}_+$ and $\boldsymbol{\Psi}_-$. Combining equations (2.12) and (2.17) into a matrix equation yields the simple form

$$\begin{pmatrix} \eta_1 e^{i\alpha(x_1-x_1)} & \dots & \eta_{n-1}e^{i\alpha(x_{n-1}-x_1)} & \eta_n e^{i\alpha(x_n-x_1)} \\ e^{i\alpha(x_1-x_2)} & 0 & 0 & 0 \\ 0 & \ddots & 0 & \vdots \\ 0 & 0 & e^{i\alpha(x_{n-1}-x_n)} & 0 \end{pmatrix} \begin{pmatrix} \Psi_+^{(1)} \\ \Psi_+^{(2)} \\ \vdots \\ \Psi_+^{(n)} \end{pmatrix} = \begin{pmatrix} \Psi_-^{(1)} \\ \Psi_-^{(2)} \\ \vdots \\ \Psi_-^{(n)} \end{pmatrix} + \begin{pmatrix} F \\ 0 \\ \vdots \\ 0 \end{pmatrix} \tag{2.18}$$

We now find a partial rearrangement of (2.18) such that unknown functions $\boldsymbol{\Psi}_\pm$ do not appear premultiplied by terms growing exponentially in $\mathcal{D}^\pm$ respectively. This may be achieved by writing equation (2.12) in terms of $\Psi_-^{(1)}, \dots, \Psi_-^{(m)}, \Psi_+^{(m)}, \dots, \Psi_+^{(n)}$ and rescaling by $e^{-i\alpha x_m}$. We so find an equation

$$\sum_{l=0}^{m-1} \eta_l(\alpha)e^{i\alpha(x_l - x_m)}\Psi_-^{(l+1)}(\alpha) + \sum_{l=m}^{n} \eta_l(\alpha)e^{i\alpha(x_l - x_m)}\Psi_+^{(l)}(\alpha) = F^{(m)}(\alpha) \tag{2.19}$$

for each m, recalling $\eta_0(\alpha) = 1$. Together these yield a matrix Wiener–Hopf equation

$$\mathbf{A}\boldsymbol{\Psi}_- + \mathbf{B}\boldsymbol{\Psi}_+ = \mathbf{F} \tag{2.20}$$

where the matrices $\mathbf{A}$ and $\mathbf{B}$ are lower and upper triangular matrices of the form

$$\mathbf{A} = \begin{pmatrix} H^{(1,1)}E^{(1,1)} & 0 & 0 \\ \vdots & \ddots & 0 \\ H^{(n,1)}E^{(n,1)} & \dots & H^{(n,n)}E^{(n,n)} \end{pmatrix}, \quad \mathbf{B} = \begin{pmatrix} G^{(1,1)}E^{(1,1)} & \dots & G^{(1,n)}E^{(1,n)} \\ 0 & \ddots & \vdots \\ 0 & 0 & G^{(n,n)}E^{(n,n)} \end{pmatrix} \tag{2.21}$$

with $G^{(l,m)} = \eta_m$, $H^{(l,m)} = \eta_{m-1}$ and $E^{(l,m)} = e^{i\alpha(x_m - x_l)}$ (so $E^{(m,m)} = 1$ for each m). Here $P^{(l,m)}$ denotes the (l,m) entry of a matrix $\mathbf{P}$. We explicitly present the case of collinear finite rigid plates in Section 3(b).

Equation (2.20) underlies a matrix Wiener–Hopf problem: find functions $\boldsymbol{\Psi}_\pm$, respectively analytic and obeying growth restrictions in $\mathcal{D}^+ = \Im(\alpha) > -c$ and $\mathcal{D}^- = \Im(\alpha) < c$, satisfying equation (2.20) on the strip $\mathcal{D}^+ \cap \mathcal{D}^- = -c < \Im(\alpha) < c$.

(c) Wiener–Hopf technique

Before discussing the iterative solution method in the next section, it is helpful to recall the standard procedure for solving Wiener–Hopf problems [1]. The first step to solving (2.20) is to find multiplicative Wiener–Hopf factorisation of $\boldsymbol{B}^{-1}\boldsymbol{A} = (\boldsymbol{K}^+)^{-1}\boldsymbol{K}^-$. We follow the convention of [20] to use upper $\pm$ indices to denote multiplicative factorisation, and lower indices for additive splittings. This facilitates a rearrangement of equation (2.20) such that all unknown functions $\boldsymbol{\Psi}_\pm$ appear within terms analytic in $\mathcal{D}^-$ or $\mathcal{D}^+$

$$\boldsymbol{K}^-\boldsymbol{\Psi}_- + \boldsymbol{K}^+\boldsymbol{\Psi}_+ = \boldsymbol{K}^+\boldsymbol{B}^{-1}\boldsymbol{F} \tag{2.22}$$

Next, additively splitting the known forcing term involving $\boldsymbol{F}$ allows for the equation to give an equality between an expression analytic in $\mathcal{D}^-$ and another analytic in $\mathcal{D}^+$

$$\boldsymbol{K}^-\boldsymbol{\Psi}_- - (\boldsymbol{K}^+\boldsymbol{B}^{-1}\boldsymbol{F})_- = -\boldsymbol{K}^+\boldsymbol{\Psi}_+ + (\boldsymbol{K}^+\boldsymbol{B}^{-1}\boldsymbol{F})_+ \tag{2.23}$$

whence analytic continuation may be used to define an entire function which may be characterised by the extended Liouville's theorem. For the scalar case, the required splittings may be expressed in terms of Cauchy transforms [1]. The additive splittings $(\cdot)_\pm$ may be accomplished by invoking the Cauchy integral formula:

$$f(\alpha) = f_+(\alpha) + f_-(\alpha) = \frac{1}{2\pi i}\int_{C_+} \frac{f(z)}{z-\alpha}\,\mathrm{d}z + \frac{1}{2\pi i}\int_{C_-} \frac{f(z)}{z-\alpha}\,\mathrm{d}z \tag{2.24}$$

where $C_\pm$ denote contours from $-\infty$ to ∞ in $\mathcal{D}^+ \cap \mathcal{D}^-$ and α lies above C_+ and below C_- [1]. Multiplicative scalar factorisations of functions with zero index along the separation contour may be obtained via additive splittings by considering the logarithm [1,43]. We recall that this approach does not generically apply to the matrix case; for instance, multiplicative factorisations may be non-commutative and there are complications associated with partial indices [7]. We now describe in Section 3 how the 'easy' solution of scalar Wiener–Hopf problems can be used to form a building block for an iterative method to attack a class of 'difficult' matrix Wiener–Hopf problems.

3. Iterative method

(a) Method

We propose an iterative method to solve matrix Wiener–Hopf problems (2.20) where the matrices $\mathbf{A}$ and $\mathbf{B}$ take the general form of (2.21) and the following constraints apply:

(i) entries in $\mathbf{H}(\alpha)$ and $\mathbf{G}(\alpha)$ have at worst pole singularities or branch cuts in $\mathbb{C}$ and at worst algebraic growth as $|\alpha| \to \infty$, and the diagonal entries $H^{(m,m)}$, $G^{(m,m)}$ have zero index
(ii) each $E^{(l,m)}$ decays exponentially in $\mathcal{D}^-$ if $l < m$, in $\mathcal{D}^+$ if $l > m$ and $E^{(m,m)} = 1$

Starting from equation (2.20) and explicitly writing the scalar equation corresponding to the m^{th} row we may find a functional equation of Wiener–Hopf type for $\Psi_{\pm}^{(m)}$

$$A^{(m,m)}\Psi_{-}^{(m)} + B^{(m,m)}\Psi_{+}^{(m)} = \tilde{F}^{(m)} \tag{3.1}$$

where $A^{(m,m)}$ and $B^{(m,m)}$ possess multiplicative Wiener–Hopf factorisations and the forcing term on the right hand side is given by

$$\tilde{F}^{(m)} = F^{(m)} - \sum_{l<m} A^{(m,l)}\Psi_{-}^{(l)} - \sum_{l>m} B^{(m,l)}\Psi_{+}^{(l)} \tag{3.2}$$

Therefore, if $\Psi_{\pm}^{(l)}$ for $l \neq m$ were known then (3.1) may be solved by the scalar Wiener–Hopf technique. The constraints on the exponential terms $E^{(l,m)}$ ensure that all terms involving exponential factors in $\tilde{F}^{(m)}$ decay in one of $\mathcal{D}^{+}$ or $\mathcal{D}^{-}$ to aid additive factorisation.

We now construct a fixed-point iteration scheme generating successive approximations $\Psi_{\pm}^{(m)r}$ to $\Psi_{\pm}^{(m)}$ by using previously obtained approximations to $\Psi_{\pm}^{(l)}$ for $l \neq m$. For instance, to find the r^{th} approximation to $\Psi_{\pm}^{(m)}$ we might solve a scalar Wiener–Hopf problem

$$A^{(m,m)}\Psi_{-}^{(m)r} + B^{(m,m)}\Psi_{+}^{(m)r} = F^{(m)} - \sum_{l<m} A^{(m,l)}\Psi_{-}^{(l)r-1} - \sum_{l>m} B^{(m,l)}\Psi_{+}^{(l)r-1} \tag{3.3}$$

The procedure may be initialised by providing an estimate for $\Psi_{\pm}^{(l)}$ for $l \neq m$. For now we suppose that each row of the matrix formulation is solved in turn (i.e. we solve (3.3) for $m = 1$ through to n in ascending order). In general the set of scalar Wiener–Hopf problems may be solved in any order, though this can affect the rate of convergence as discussed in Section 5(b). In this paper the initial estimate for $\Phi_{\pm}^{(l)}$ for all $l \neq m$ is taken to be 0, which corresponds to neglecting any exponential terms in equation (3.3), and hence any coupling of the off-diagonal elements of $\mathbf{A}$ and $\mathbf{B}$ in (2.20).

This method is inspired by the earlier work [20] that considers rearrangements of a 2×2 matrix Wiener–Hopf problem so as to justify initially neglecting terms involving exponential factors. Here, we initially neglect terms involving exponential factors following a partial rearrangement to ensure exponential factors decay in the relevant regions of the complex plane; this is associated with the idea that the coupling with the neglected terms is weak. We note that a numerical approach to solve Riemann–Hilbert problems involving exponential factors proposed previously [24] also uses iteration, though does not employ the scalar Wiener–Hopf technique and appeal to Liouville's theorem; understanding the relationship between these approaches offers an interesting avenue for future study.

Importantly, the procedure described has reduced the matrix Wiener–Hopf problem to a system of successive scalar Wiener–Hopf problems which may be solved via Cauchy transforms. These transforms are implemented numerically as later described in Section 3(c).

(b) Example: Collinear finite rigid plates

Having illustrated how matrix Wiener–Hopf problems of the form (2.20)-(2.21) can arise from mixed boundary value problems, we now explicitly consider the example of N collinear finite plates to further clarify the method. Defining V_m and $\boldsymbol{\Psi}_{\pm}$ according to equations (2.14) and (2.17) respectively we find

$$\mathbf{A} = \begin{pmatrix} 1 & & & \\ e^{i\alpha(x_1-x_2)} & \gamma(\alpha) & & \\ \vdots & & \ddots & \\ e^{i\alpha(x_1-x_n)} & \gamma(\alpha)e^{i\alpha(x_2-x_n)} & \cdots & \gamma(\alpha) \end{pmatrix} \tag{3.4a}$$

$$\mathbf{B} = \begin{pmatrix} \gamma(\alpha) & e^{i\alpha(x_2-x_1)} & \cdots & e^{i\alpha(x_n-x_1)} \\ & 1 & \cdots & e^{i\alpha(x_n-x_2)} \\ & & \ddots & \vdots \\ & & & 1 \end{pmatrix} \tag{3.4b}$$

$$F^{(m)} = -ik\sin\theta_i e^{-i\alpha x_m} \sum_{l=1}^{N} \frac{e^{i(\alpha+k_x)x_{2l-1}} - e^{i(\alpha+k_x)x_{2l}}}{\alpha + k_x}, \tag{3.4c}$$

where $k_x = -k\cos\theta_i$ and we recall that $\gamma(\alpha) = \sqrt{i(\alpha-k)}\sqrt{-i(\alpha+k)}$.

The initial guesses of the off-diagonal terms are 0, so the approximations in first iteration may be found by solving

$$\Psi_-^{(m)0}(\alpha) + \gamma(\alpha)\Psi_+^{(m)0}(\alpha) = F^{(m)}(\alpha) - \sum_{l<m} A^{(m,l)}\Psi_-^{(l)0} \tag{3.5}$$

in the order $m = 1, \ldots, n$. Then subsequent terms could be given by solving at the r^{th} iteration

$$\Psi_-^{(m)r}(\alpha) + \gamma(\alpha)\Psi_+^{(m)r}(\alpha) = F^{(m)}(\alpha) - \sum_{l<m} A^{(m,l)}\Psi_-^{(l)r} - \sum_{l>m} B^{(m,l)}\Psi_+^{(l)r-1} \tag{3.6}$$

for $m = 1, \ldots, n$. The scalar Wiener–Hopf problem at each iteration resembles that for the classical Sommerfeld half-plane problem, albeit with modified forcing; for instance, taking m odd we have

$$\Psi_-^{(m)}(\alpha) + \gamma(\alpha)\Psi_+^{(m)}(\alpha) = \tilde{F}^{(m)}(\alpha) \tag{3.7}$$

This is of a form that may be associated with scattering by a semi-infinite rigid plate on $[0, \infty]$. Considering equation (3.7), the iterative method for the case of collinear plates may be interpreted as constructing a Schwarzschild diffraction series in the spectral domain, each iteration corresponding to a diffraction event [44].

For the problems in this paper, as in the classical half-plane problem, when appealing the Liouville's theorem the entire functions are found to be identically zero by considering the large $|\alpha|$ behaviour of the known and unknown Fourier transforms [1]. In order to apply the iterative procedure, we take the inital estimates of the unknown functions to be zero as mentioned previously, and we are left to choose an order in which to solve these scalar equations to provide a fixed-point iterative method; we will discuss the order chosen in Section 5(b). To apply the method to the alternative geometries (b) and (c) involving semi-infinite plates the only noteworthy point is that care must be taken over the location of poles associated with the reflected field when performing additive factorisations (for case (a) of finite plates all forcing functions are entire).

(c) Numerical implementation

The iterative solution method described in the previous section involves solving a sequence of scalar Wiener–Hopf problems. We therefore require an effective means to compute the Cauchy transforms associated with the necessary additive splittings described in equation (2.24). Practical limitations to two or three iterations, as faced in [27], may be overcome by automating the procedure. To numerically compute Cauchy transforms efficiently we employ the approach proposed in [31]. First the function of interest is represented in a basis encoding singular endpoint behaviour. Known analytic expressions for the Cauchy transforms of these basis functions may then be used to find the required moments. This can provide a spectrally accurate approximation to the Cauchy transform throughout the complex plane, notably mitigating errors near the contours of integration typically associated with computing singular integrals.

For the problems considered in this paper, recall that the relevant scalar Wiener–Hopf problems have kernel $\gamma(\alpha)$ with multiplicative factors $\gamma_\pm(\alpha) = \sqrt{\mp i(\alpha \pm k)}$. We so require additive factorisations of expressions of the form $f_\mp/\gamma_\pm$. We take care to compute the

factorisation via a Cauchy integral in the half-plane where f decays. For example, given a function

$$f(\alpha) = \frac{1}{\gamma_-(\alpha)} \left(\frac{e^{i(\alpha+k_x)L} - 1}{\alpha + k_x} \right) \tag{3.8}$$

with $L > 0$ we find the additive Wiener–Hopf splitting by first computing

$$f_-(\alpha) = \left(\frac{1}{\gamma_-(\alpha)} \left(\frac{e^{i(\alpha+k_x)L} - 1}{\alpha + k_x} \right) \right)_- = \frac{1}{2\pi i} \int_{C_-} \frac{f(z)}{z - \alpha} \, \mathrm{d}z \tag{3.9}$$

recalling the contours $C_\pm$ from equation (2.24), and recover f_+ using the equality $f_+(\alpha) = f(\alpha) - f_-(\alpha)$, thus avoiding the exponential growth of f in the lower half-plane.

To compute the Cauchy transform efficiently we first deform the contour C_+ or C_- onto the branch cut in the appropriate half-plane, perhaps picking up contributions from residues. the branch cuts of γ are intentionally taken to be parallel to the imaginary axis to be paths of steepest descent of the exponential factors $e^{i\alpha x_m}$. Considering each side of the semi-infinite branch cut separately, we find induced square root endpoint singularities in f at the branch points. Each Cauchy transform to be computed so takes the form

$$\frac{1}{2\pi i} \int_0^\infty \frac{g(x)}{x^{1/2}(x - z)} \, \mathrm{d}x \tag{3.10}$$

where g is a smooth non-oscillatory function decaying as $x \to \infty$. Next, the Cauchy transform along $(0, \infty)$ may be related to the canonical interval $(-1, 1)$ using the Möbius transform

$$x = M(s) = \lambda \left(\frac{1 + s}{1 - s} \right) \tag{3.11}$$

Cauchy transforms under change of variables by Möbius mappings may be related using Plemelj's lemma [22,32], or by explicity considering the change of variables. We find that (3.10) may be computed via

$$\int_0^\infty \frac{g(x)}{x^{1/2}(x - z)} \, \mathrm{d}x = \int_{-1}^1 \frac{h(s)}{s - M^{-1}(z)} \, w(s) \mathrm{d}s - \int_{-1}^1 \frac{h(s)}{s - 1} \, w(s) \mathrm{d}s \tag{3.12}$$

where $h(s) = \lambda^{-1/2}(1 - s)g(M(s))$ is a smooth non-oscillatory function decaying as $s \to 1$ and $w(s) = (1 - s)^{-1/2}(1 + s)^{-1/2}$. We now approximate the mapped function $h(s)$ on $(-1, 1)$ by expanding in Chebyshev polynomials of the first kind T_j:

$$h(s) = \sum_{j=0}^{n_c - 1} a_j T_j(s) \tag{3.13}$$

where n_c is the number of basis functions used; the coefficients a_j may be found via fast transforms available in ApproxFun.jl [45]. The Cauchy transform (3.10) may then be computed via a related basis, the 'vanishing basis' of Chebyshev polynomials of the first kind, given by

$$T_0^z(s) = 1, \quad T_1^z(s) = s, \quad T_j^z(s) = T_j(s) - T_{j-2}(s), \quad \text{for } j \geq 2 \tag{3.14}$$

whose Cauchy transforms against the weight $w(s)$ take the particularly simple form

$$\frac{1}{2\pi i} \int_{-1}^1 \frac{T_j^z(s)}{s - \alpha} \, w(s) \mathrm{d}s = i \left(J_+^{-1}(\alpha) \right)^{j-1} \qquad j \geq 2 \tag{3.15}$$

where $J_+^{-1}(z) = z - \sqrt{z - 1}\sqrt{z + 1}$ is one of the right inverses of the Joukowsky map [22]. Finally, the Cauchy transform (3.12) may be computed approximately by contracting the moments (3.15) with a vector of modified coefficients.

The iterative method has been implemented in Julia using ApproxFun.jl [45] and SingularIntegralEquations.jl [33,46]. By precomputing the moments of the Cauchy transforms evaluated at points of interest the associated computational expense may be decoupled from the iterative procedure. To quantify the numerical performance we define a

measure of the discrete error for an approximation f_- against a converged reference value f_-^{ref} found by considering a larger number of degrees of freedom. We compare the functions at points $\alpha_{\text{dir}} = \{-k\cos\theta \,|\, \theta \in \Theta\}$ where Θ is a set of 100 equally spaced points in $[0.001\pi, 0.999\pi]$, of later relevance to evaluating the magnitude of the scattered field in the far-field D_∞ for observer angles θ.

$$E_c = \sqrt{\sum_{\alpha\in\alpha_{\text{dir}}} \left| \frac{f_-(\alpha) - f_-^{\text{ref}}(\alpha)}{f_-^{\text{ref}}(\alpha)} \right|^2} \tag{3.16}$$

Figure 2 presents the numerical convergence for the factorisation of the typical forcing function

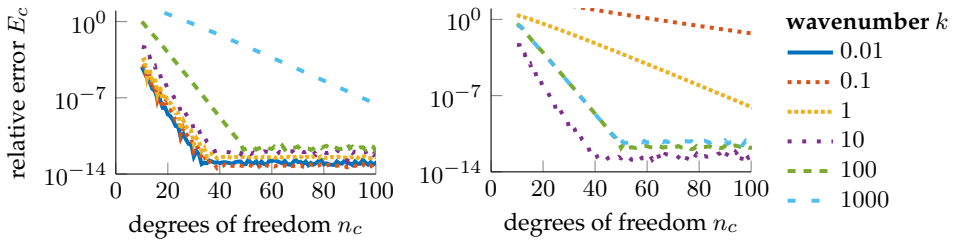

Figure 2: Convergence of Cauchy transform for f_- (equation (3.9)); in the left panel we take $\lambda = 10$, and in the right panel tailor the mapping to each term in (3.17) as described in the text

(3.8) with $L = 1$ and $k_x = -k\cos 3\pi/4$ for various wavenumbers k, in the left panel taking $\lambda = 10$. The non-uniformity in accuracy with k may be associated with the approximation of

$$(1-s)g(M(s)) = \frac{(1-s)e^{i(k+k_x)L - \lambda L\left(\frac{1+s}{1-s}\right)}}{k+k_x+i\lambda\left(\frac{1+s}{1-s}\right)} - \frac{1-s}{k+k_x+i\lambda\left(\frac{1+s}{1-s}\right)} \tag{3.17}$$

on $(-1, 1)$. Convergence may be tuned by exploiting the free mapping parameter λ and the non-dimensionalisation scaling kL. For instance, taking $\lambda = 1$ for first term in (3.17), but $\lambda = k$ for the second term we observe that it appears possible to minimise wavenumber dependence for large wavenumbers, as demonstrated in the right panel of figure 2.

More generally, it is useful to note that the spectral approach to compute Cauchy transforms may be implemented for a variety of asymptotic function behaviours and contours by using known formulae for Cauchy transforms of various basis functions, including orthogonal polynomials against their weights, and exploiting the relationships between Cauchy transforms under rational mappings [22–24,32,47].

4. Results

In this section we explore the method by considering scattering of plane waves by a set of collinear plates in two dimensions in each of the distinct cases shown in figure 1.

(a) Scattering from a finite plate

To first validate our implementation we consider scattering by a single finite rigid plate which is associated with a 2×2 matrix Wiener–Hopf equation. In figure 3 we plot the far-field directivity D_∞ as defined in equation (2.10) for a plane wave incident at an angle $\theta_i = \pi/4$ with $L = 1$ and $kL = 12$, computed using the method of steepest as given in [27] and the 'exact' Mathieu function solution presented therein. We may recover the directivity D_∞ from $\Psi_+^{(0)r}$ or $\Psi_-^{(1)r}$, where the index r denotes the r^{th} approximation to the quantity, starting at $r = 0$. The iterative method converges by eye to the exact solution after four iterations (0,1,2,3), taking approximately 0.1s

on a 2018 Macbook Pro with a 2.3GHz i5 processor and 8GB ram. Convergence of the iterative method will be considered in more detail in Section 5.

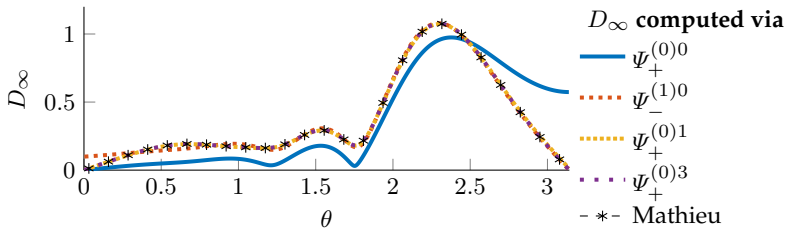

Figure 3: Comparison of far-field directivity D_∞ for scattering a plane wave incident at an angle $\theta_i = \pi/4$ by a single finite rigid plate for $L = 1$, $kL = 12$, between Mathieu function expansion derived for [27] and our numerical implementation

(b) Scattering from a screen

The formulation of the matrix Wiener–Hopf system presented in Section 2(b) allows for an arbitrary number of plates, and may be naturally adapted to case (c) of scattering by a set of apertures in a rigid screen as pictured in figure 1c. We consider scattering from a set of apertures in a doubly infinite screen and demonstrate the near-field spatial inversion of the field, computed numerically from the inverse Fourier transform. We reproduce a case from [40] where a screen is considered with apertures at $[0, 2\pi]$, $[2.1\pi, 2.5\pi]$, $[2.8\pi, 3.5\pi]$, $[4\pi, 6\pi]$, $[6.1\pi, 10\pi]$ and $k = 5$. Figure 4 presents our results which show close agreement with that produced in panel (a) of figure 2 in [40].

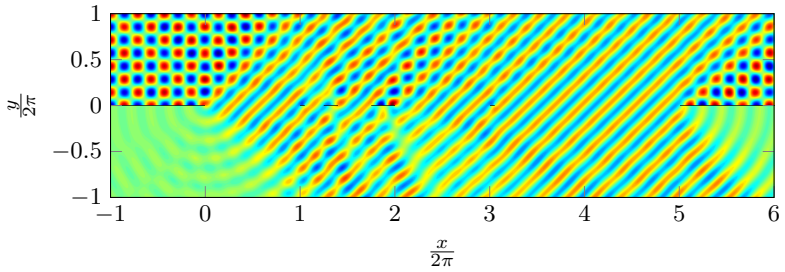

Figure 4: Real part of the total field $\phi + \phi_i$ for a plane wave of wavenumber $k = 5$ incident at an angle $\theta_i = 3\pi/4$ on five apertures at $[0, 2\pi]$, $[2.1\pi, 2.5\pi]$, $[2.8\pi, 3.5\pi]$, $[4\pi, 6\pi]$, $[6.1\pi, 10\pi]$ in an otherwise infinite rigid plate. This reproduces panel (a) of figure 2 in [40]; the x and y axes are scaled by a factor of 2π to facilitate comparision.

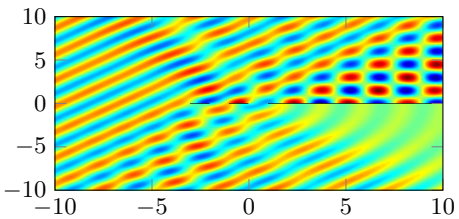

Figure 5: Real part of the total field $\phi + \phi_i$ for a plane wave of wavenumber $k = 3$ incident at angle $\theta_i = 3\pi/4$ on a semi-infinite plate on the interval $[1, \infty]$ and finite plates at $[-3, -2]$ and $[-1, 0]$

(c) Scattering from a semi-infinite plate with grated extension

We now consider the problem of scattering from a semi-infinite geometry, case (b), as pictured in figure 1b. In figure 5 we present the near field for scattering a plane wave of wavenumber $k = 3$ incident at angle $\theta_i = 3\pi/4$ by a semi-infinite rigid plate on the interval $[1, \infty]$ and two finite rigid plates at $[-3, -2]$ and $[-1, 0]$. We remark that the only notable difference when applying the iterative method to this example is the need to remove the pole when undertaking Wiener–Hopf factorisations.

Whilst such problems are ideally suited to the Wiener–Hopf technique, boundary element methods can become difficult as the integral formulations require care when posed on infinite intervals and an appropriate choice of basis functions must be made. For a finite set of apertures, as pictured in figure 1c, the problem may be recast as a modified problem posed on a finite boundary formed by the apertures, as in [40]. By contrast, for geometries involving precisely one semi-infinite plate such a rearrangement again leads to a problem posed on an infinite interval.

5. Convergence

We now investigate the convergence of the iterative scheme with iteration number. By a single iteration we mean solving one Wiener–Hopf equation for each junction. We define an error measure for an approximation Φ^r to Φ, found by terminating the iterative method after r iterations, against a reference solution Φ^{ref}

$$E_\Phi = \sqrt{\sum_{\alpha \in \alpha_{\text{dir}}} \left| \frac{\Phi^r(\alpha) - \Phi^{\text{ref}}(\alpha)}{\Phi^{\text{ref}}(\alpha)} \right|^2} \tag{5.1}$$

where the points α_{dir} are as in (3.16), corresponding to evaluating the far-field directivity D_∞ at 100 equally spaced angles $\{0.001\pi, \ldots, 0.999\pi\}$. The reference solution Φ_{ref} is taken to be a converged solution provided by terminating the iterative sequence at a larger number of iterations. The complexity of the numerical scheme is predominantly associated with the number of *scalar factorisations* C_{factor} to be undertaken. This is given by the product of the number of junctions n and the number of *iterations* C_{it}, $C_{\text{factor}} = nC_{\text{it}}$. In all cases we consider an incident plane wave at angle $\theta_i = \pi/4$.

(a) Finite plate

We first consider the simplest case of scattering by a single finite rigid plate. Figure 6a presents the relative error E_Φ at each iteration for a range of Helmholtz numbers kL. Each iteration successively improves the solution; further, the solution of each scalar problem most significantly corrects the directivity in the direction away from the junction that scalar problem may be associated with (i.e. towards $\theta = 0$ having solved for the extreme right hand junction at $x = L$ and $\theta = \pi$ after solving for the left hand junction at $x = 0$), as discussed in [27]. This may be most clearly seen in figure 6b where we plot the pointwise relative error in the directivitity for each angle θ at successive iterations. The procedure converges geometrically with iteration number, interestingly even when the plate Helmholtz number kL is smaller than unity. This has a physical interpretation: each iteration accounts for an additional backscattering between junctions. On physical grounds the backscattered field is expected to be weaker than the incident field that induced it; if this proportion may be bounded above by a constant less than one then geometric convergence would be anticipated regardless of Helmholtz number.

(b) Iteration sequence for $n \times n$ problems

The iterative procedure centres on the sequential solution of scalar Wiener–Hopf problems corresponding to the rows of the matrix equation (2.20); the sequence in which these problems

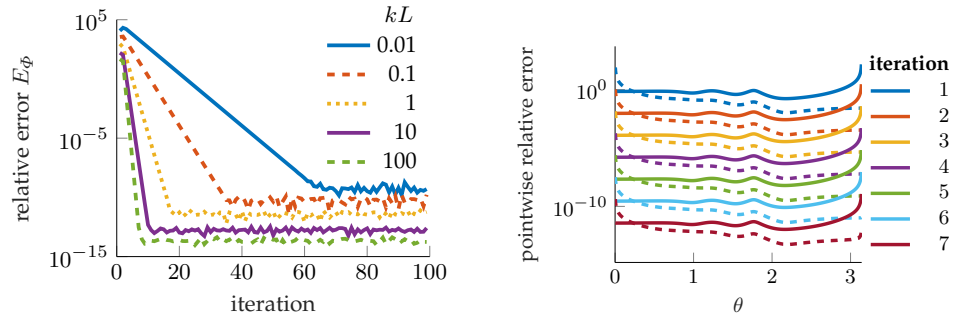

(a) Convergence for various wavenumbers

(b) Error in far-field directivity $D_\infty(\theta)$

Figure 6: Convergence in iteration for scattering by a finite plate. In panel (a) we observe faster convergence for higher wavenumbers. Panel (b) takes $kL = 12$ and considers the pointwise relative error in D_∞ after each scalar Wiener–Hopf problem has been solved, including a partial update at each 'half-iteration'. The error is greatest in direction $\theta = 0$ or π away from the junction most recently solved: after solving for the junction at $x = L$ (solid) and $x = 0$ (dashed) respectively.

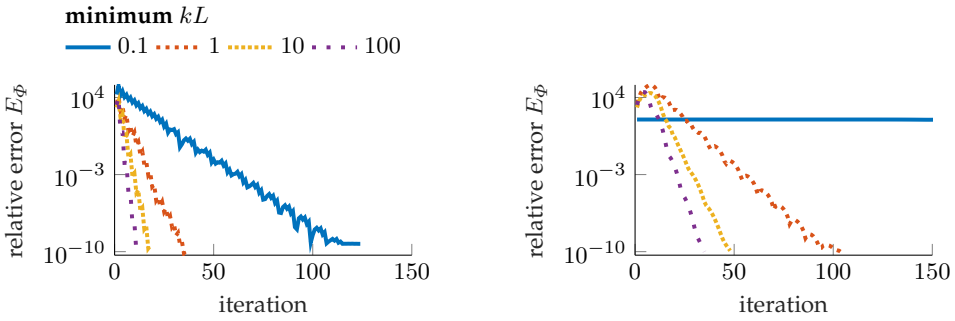

(a) FB - forwards-backwards sequence

(b) FF - forwards-forwards sequence

Figure 7: Comparison of iteration strategies for 5 plates of unit length with unit spacing considering a plane wave incident at an angle $\theta_i = \pi/4$ for various wavenumbers k. Iterating forward then back (FB) is consistently preferable to only passing through the system forwards (FF), and for low wavenumbers the FF strategy may not converge

are solved may be chosen in various ways. To investigate this choice we consider the problem of scattering by a set of 5 unit length, unit spaced rigid plates for wavenumbers $k = 0.1, 1, 10, 100$.

Figure 7 presents convergence results for two strategies: forward-backward (FB), in which the equations are solved in the repeated pattern $1, 2, \ldots, n-1, n, n-1, \ldots, 2, 1$, shown in panel (a), and forward-forward (FF) in which the equations are solved by the repeated pattern $1, 2, \ldots, n, 1, 2, \ldots, n$, shown in panel (b). In all cases the FB strategy, in which adjacent junctions are solved for sequentially, converges faster that the FF strategy. Further, the FF strategy does not even appear to converge in the 'hardest' case presented of $k = 0.1$, though applying the FB strategy does converge. That the FB strategy often appears optimal may be understood as follows: each Wiener–Hopf problem solves for Fourier transforms of adjacent unknown boundary values. Each such unknown is most strongly coupled to the values on the boundary sections in closest proximity. By always solving Wiener–Hopf problems associated with adjacent junctions successively, we always update the values anticipated to change most due to previous updates.

(c) Convergence wavenumber dependence

Now that we have established a heuristic to choose the sequence in which to apply the iterative scheme, we consider the convergence of the scheme for different wavenumbers.

The method is anticipated to be best suited to large wavenumbers, or more precisely scattering problems for which the minimum Helmholtz number is large. This ensures that the backscattering effects between each junction are indeed small. Figure 8a considers scattering from a set of $1, 5, 10$ and 20 collinear unit spaced unit length rigid plates and presents the number of iterations to find 5 s.f. of accuracy against smallest Helmholtz number, $\min kL$, where L is a lengthscale associated with the geometry. For mid to high wavenumbers the number of iterations required is very small, often less than 20, broadly independent of the size of the system. The number of factorisations to achieve a given accuracy so scales at worst quadratically with the number of junctions n, as each iteration requires the solution of n scalar Wiener–Hopf equations, each of which has $\mathcal{O}(n)$ terms to be factorised. For $\min kL < 1$ the number of iterations to achieve a given accuracy increases rapidly with reducing wavenumber, and more iterations are required for larger n. To investigate

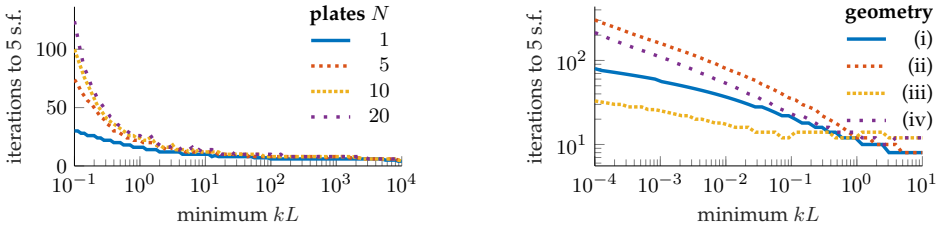

(a) Large Helmholtz number convergence for a range of numbers of plates

(b) Small Helmholtz number convergence for various configurations (i)-(iv) described below

Figure 8: Number of iterations required to achieve 5 s.f. of accuracy in D_∞ against minimum Helmholtz number kL associated with the scattering problem. Geometries considered in panel (b) are (i) - finite plate length L, (ii) - two finite plates length L and spacing L, (iii) - two finite plates length 1 and spacing L and (iv) - two finite plates of length 1 and L respectively, spacing 1

this low wavenumber performance we consider a range of different scattering problems involving one or two finite plates. Figure 8b shows the number of iterations required to achieve 5 s.f. of accuracy and appears to demonstrate that the number of iterations required grows at worst algebraically with the inverse of $\min kL$.

6. Conclusion

This paper has demonstrated the efficacy of iteration to solve a class of $n \times n$ matrix Wiener-Hopf problems involving exponential factors by leveraging scalar techniques, extending the approach of [20,27] based upon physically motivated scalar subsystems. This enables the extension of (semi-)analytic techniques to scattering from problems involving multiple junctions, as we show through the example of scattering from many collinear plates. Convergence is demonstrated even at small reduced wavenumbers. Exploiting spectral representations to accurately evaluate the (singular) Cauchy transforms generates a fast and accurate numerical scheme. Results have been validated against existing approaches.

The use of iteration is most appealing in cases where there is a clear separation of scales yielding a hierarchical structure within the system, as occurs for large reduced wavenumbers, and problems for which alternative solution methods are unsuitable, such as non-linear systems. The ability to deal with a large number of junctions may make this technique appropriate for the study of subfractal geometries associated with metamaterials [48], or models of perforated surfaces [49]. Iteration based on carefully chosen subproblems promises a useful tool to extend numerous existing Wiener-Hopf treatments of fundamental problems with physical interest.

Data Accessibility. This work has no additional data.

Authors' Contributions. M.J.P. produced and analysed the numerical implementation and results. M.J.P. and A.V.K. derived the mathematical model and its solution. All authors contributed to the writing of the manuscript and gave final approval for publication.

Competing Interests. The authors declare that they have no competing interests.

Funding. This work was supported by EPSRC DTP EP/N509620/1 (M.J.P.), the Sultan Qaboos Research Fellowship at Corpus Christi College at University of Cambridge (A.V.K.) and by EPSRC early career fellowship EP/P015980/1 (L.J.A.). The authors would like to thank the Isaac Newton Institute for Mathematical Sciences, Cambridge, for support and hospitality during the WHT programme where some work on this paper was undertaken (EPSRC grant no EP/R014604/1).

Acknowledgements. M.J.P. thanks Sheehan Olver for advice to use SingularIntegralEquations.jl, Elena Luca, David Hewett and David Baker for discussions during the completion of this work and Matthew Colbrook for sharing code to compute the single plate Mathieu function solution. A.V.K. thanks Andrey Shanin for useful discussions. Numerous comments by anonymous referees helped to improve this paper.

References

1. Noble B. 1988 *Methods based on the Wiener-Hopf technique for the solution of partial differential equations*. Chelsea Pub Co.
2. Veitch BH, Peake N. 2008 Acoustic propagation and scattering in the exhaust flow from coaxial cylinders. *J. Fluid Mech.* **613**, 275–307.
3. Tymis N, Thompson I. 2014 Scattering by a semi-infinite lattice and the excitation of Bloch waves. *The Quarterly Journal of Mechanics and Applied Mathematics* **67**, 469–503.
4. Balmforth NJ, Craster RV. 1999 Ocean waves and ice sheets. *J. Fluid Mech.* **395**, 89–124.
5. Mishuris GS, Movchan AB, Slepyan LI. 2008 Dynamics of a bridged crack in a discrete lattice. *Quart. J. Mech. Appl. Math.* **61**, 151–160.
6. Green R, Fusai G, Abrahams ID. 2010 The Wiener-Hopf technique and discretely monitored path-dependent option pricing. *Math. Finance* **20**, 259–288.
7. Mishuris GS, Rogosin S. 2016 Factorization of a class of matrix-functions with stable partial indices. *Mathematical Methods in the Applied Sciences* **39**, 3791–3807.
8. Rogosin S, Mishuris GS. 2016 Constructive methods for factorization of matrix-functions. *IMA Journal of Applied Mathematics* **81**, 365–391.
9. Mishuris G, Rogosin S. 2018 Regular approximate factorization of a class of matrix-function with an unstable set of partial indices. *Proc. Roy. Soc. London Ser. A* **474**, 20170279.
10. Crighton DG, Leppington FG. 1970 Scattering of aerodynamic noise by a semi-infinite compliant plate. *Journal of Fluid Mechanics* **43**, 721–736.
11. Mishuris GS, Rogosin S. 2014 An asymptotic method of factorization of a class of matrix functions. *Proc. Roy. Soc. London Ser. A* **470**.
12. Abrahams ID. 2000 The application of Pade approximants to Wiener-Hopf factorization. *IMA Journal of Applied Mathematics* **65**, 257–281.
13. Idemen M. 1979 A New Method to Obtain Exact Solutions of Vector Wiener-Hopf Equations. *ZAMM - Zeitschrift für Angewandte Mathematik und Mechanik* **59**, 656–658.
14. Abrahams ID. 1987 Scattering of sound by two parallel semi-infinite screens. *Wave Motion* **9**, 289 – 300.
15. Lawrie JB, Abrahams ID. 2007 A brief historical perspective of the Wiener-Hopf technique. *J. Engrg. Math.* **59**, 351–358.
16. Antipov YA. 2010 A symmetric Riemann-Hilbert problem for order-4 vectors in diffraction theory. *Quart. J. Mech. Appl. Math.* **63**, 349–374.
17. Jones DS. 1984 Commutative Wiener-Hopf factorization of a matrix. *Proc. Roy. Soc. London Ser. A* **393**, 185–192.
18. Primachuk L, Rogosin S. 2018 Factorization of Triangular Matrix-Functions of an Arbitrary Order. *Lobachevskii Journal of Mathematics* **39**, 129–137.
19. Abrahams ID, Wickham GR. 1990 General Wiener-Hopf Factorization of Matrix Kernels with Exponential Phase Factors. *SIAM Journal on Applied Mathematics* **50**, 819–838.
20. Kisil AV. 2018 An Iterative Wiener–Hopf Method for Triangular Matrix Functions with Exponential Factors. *SIAM Journal on Applied Mathematics* **78**, 45–62.
21. Antipov YA. 2015 Vector Riemann–Hilbert problem with almost periodic and meromorphic coefficients and applications. *Proc. Roy. Soc. London Ser. A* **471**, 20150262.

22. Trogdon T, Olver S. 2016 *Riemann–Hilbert Problems, Their Numerical Solution, and the Computation of Nonlinear Special Functions*. SIAM.
23. Llewellyn Smith SG, Luca E. 2019 Numerical solution of scattering problems using a Riemann–Hilbert formulation. *Proc. Roy. Soc. London Ser. A* **475**, 20190105.
24. Trogdon T. 2015 On the application of GMRES to oscillatory singular integral equations. *BIT Numerical Mathematics* **55**, 591–620.
25. Veitch BH, Abrahams ID. 2007 On the commutative factorization of $n \times n$ matrix Wiener-Hopf kernels with distinct eigenvalues. *Proc. R. Soc. Lond. Ser. A Math. Phys. Eng. Sci.* **463**, 613–639.
26. Erbaş B, Abrahams ID. 2007 Scattering of sound waves by an infinite grating composed of rigid plates. *Wave Motion* **44**, 282–303.
27. Kisil AV, Ayton LJ. 2018 Aerodynamic noise from rigid trailing edges with finite porous extensions. *Journal of Fluid Mechanics* **836**, 117–144.
28. Livasov P, Mishuris GS Numerical factorisation of a matrix-function with exponential factors in a problem for crack with process zone. Preprint.
29. Slepyan LI. 2002 *Models and Phenomena in Fracture Mechanics*. Springer, Berlin, Heidelberg.
30. Nieves M, Movchan A, Jones I, Mishuris G. 2013 Propagation of Slepyan's crack in a non-uniform elastic lattice. *Journal of the Mechanics and Physics of Solids* **61**, 1464 – 1488.
31. Olver S. 2011 Computing the Hilbert transform and its inverse. *Math. Comp.* **80**, 1745–1767.
32. Olver S. 2014 Change of variable formulas for regularizing slowly decaying and oscillatory Cauchy and Hilbert transforms. *Analysis and Applications* **12**, 369–384.
33. Slevinsky RM, Olver S. 2017 A fast and well-conditioned spectral method for singular integral equations. *Journal of Computational Physics* **332**, 290–315.
34. Millar RF. 1958 Diffraction by a wide slit and complementary strip. I. *Mathematical Proceedings of the Cambridge Philosophical Society* **54**, 1.
35. Grinberg GA. 1957 On a new method for the solution of the electromagnetic waves diffraction problem for a plane with an infinite rectilinear slit and for related problems. *Zhurnal Tekhnicheskoi Fiziki 27, no. 11* pp. 2565–2605. English translation published by: Soviet Physics-Technical Physic.
36. Nigro D. 2017 *Prediction of Broadband and hydrodynamic noise: derivation of analytical models for low frequency*. PhD thesis University of Manchester.
37. Popple DF, Leppington FG. 1995 The Two-Dimensional Sound Field Due to a Pair of Interacting Compliant Pistons. *Proceedings: Mathematical and Physical Sciences* **450**, 513–536.
38. Idemen M, Alkumru A. 2000 A generalization of the Wiener-Hopf approach to direct and inverse scattering problems connected with non-homogeneous half-spaces bounded by n-part boundaries. *Quart. J. Mech. Appl. Math.* **53**, 393–420.
39. Shinbrot M. 1970 The Solution of Some Integral Equations of Wiener-Hopf Type. *Quarterly of Applied Mathematics* **28**, 15–36.
40. Hewett DP, Langdon S, Chandler-Wilde SN. 2015 A frequency-independent boundary element method for scattering by two-dimensional screens and apertures. *IMA Journal of Numerical Analysis* **35**, 1698–1728.
41. Colbrook MJ, Ayton LJ, Fokas AS. 2019 The unified transform for mixed boundary condition problems in unbounded domains. *Proc. Roy. Soc. London Ser. A* **475**, 20180605.
42. Shanin AV. 2003 Diffraction of a Plane Wave by Two Ideal Strips. *The Quarterly Journal of Mechanics and Applied Mathematics* **56**, 187–215.
43. Kisil AV. 2016 *Approximate Wiener–Hopf Factorisation with Stability Analysis*. PhD Thesis University of Cambridge.
44. Shanin AV. 2003 Diffraction on a Slit: Some Properties of Schwarzschild's Series. *Journal of Mathematical Sciences* **117**, 4034–4048.
45. Olver S, Goretkin G, Slevinsky RM, Townsend A ApproxFun.jl. `https://github.com/ApproxFun/ApproxFun.jl`, GitHub.
46. Olver S, Slevinsky RM SingularIntegralEquations.jl. `https://github.com/ApproxFun/SingularIntegralEquations.jl`, GitHub.
47. Antipov YA, Mkhitaryan SM. 2018 Integral relations associated with the semi-infinite Hilbert transform and applications to singular integral equations. *Q. Appl. Math.* **76**, 739–766.
48. Chandler-Wilde SN, Hewett DP. 2018 Well-posed PDE and integral equation formulations for scattering by fractal screens. *SIAM Journal on Mathematical Analysis* **50**, 677–717.
49. Leppington FG. 1977 The effective compliance of perforated screens. *Mathematika* **24**, 199–215.